ELECTRONIC SUPPLEMENTARY INFORMATION

Role of fast dynamics in the complexation of G-quadruplexes with small molecules

Luca Bertini,[a] Valeria Libera,[a,b] Francesca Ripanti,[a] Tilo Seydel,[c] Marco Paolantoni,[d] Andrea Orecchini,[a] Caterina Petrillo,[a] Lucia Comez,[b] and Alessandro Paciaroni[a]

1 FTIR spectroscopy

FTIR spectroscopy is a vibrational spectroscopy technique that has proved to be suitable for the study of structural properties and interactions of nucleic acids. In particular, several bands assigned to specific guanine vibrations might be employed to probe local hydrogen bonding interactions and the formation of tetraplexes [*M.R. Guzmán et al., Spectrochimica Acta Part A: Molecular and Biomolecular Spectroscopy, 2006, 64, 495–503*].

In this work, we carried out FTIR experiments in Attenuated Total Reflection (ATR) mode on Tel22, Tel22-Berberine, and Tel22-BRACO19 hydrated powders. The ATR-FTIR spectra were recorded with a FTIR Bruker spectrometer (mod. Alpha-P), equipped with a Platinum ATR module employing a single reflection (45°) diamond crystal. Each spectrum was obtained at room temperature, averaging over 120 scans at a resolution of 2 cm^{-1}, using the spectrum of the empty ATR plate as the reference background. Spectral profiles in the frequency range 380–5000 cm^{-1} were converted using the “extend ATR correction” routine implemented in the Opus 7.5 Bruker Optics software. The measurements were performed at ambient conditions, at an estimated hydration of 0.13 g H_2O/g dried Tel22.

Fig. S1 shows the IR spectra recorded in the region where the most notable vibration frequencies are found in G-quadruplex structures[?]. All the spectra show the presence of the band at around 1480 cm^{-1}, which can be assigned to a vibration involving the guanine N7C8H bending motion when the N7 atom participates to Hoogsteen hydrogen bonds[?], thus confirming the formation of tetraplexes in our samples.

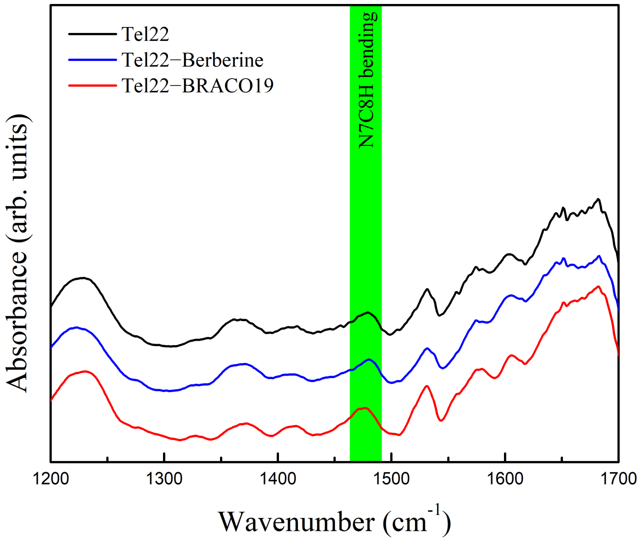

Fig. S1 Infrared spectra of Tel22 alone (black), Tel22-Berberine (blue), and Tel22-BRACO19 (red). The green bar highlights the peak associated to the formed G4 structures. In the inset the second derivative of each spectrum is shown.

2 Fit procedure of QENS data

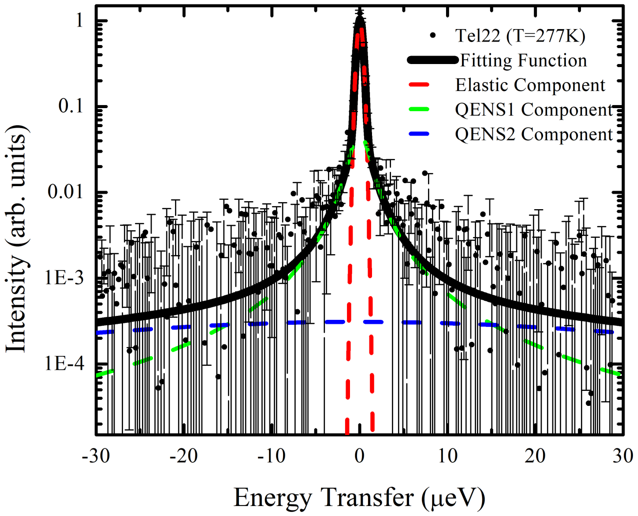

Fig. S2 QENS spectrum of Tel22 at 277 K along with the components of the fitting function 1.

QENS data were fitted through a careful procedure consisting of different steps. A preliminary analysis of the spectra found the Lorentzian broadening of the second Voigt function to be a constant function of Q and T, taking the same value $\Gamma_2 = 20\ \mu\mathrm{eV}$ for all the samples; this value was thus fixed to reduce the number of independent fit parameters. Subsequently, we fitted the spectra using this relation:

$$S(Q,\omega) = A(Q)g(\omega) + B(Q)V_1(\omega,\Gamma_1) + C(Q)V_2(\omega,\Gamma_2) \quad (1)$$

with A, B, C, and Γ_1 as independent parameters, while keep-

---

[a] *Department of Physics and Geology, University of Perugia,Via Alessandro Pascoli, 06123 Perugia, Italy*

[b] *Istituto Officina dei Materiali-IOM, National Research Council-CNR, Via Alessandro Pascoli, 06123 Perugia, Italy*

[c] *Institut Max von Laue - Paul Langevin (ILL) 71 avenue des Martyrs, 38042 Grenoble, France*

[d] *Department of Chemistry, Biology and Biotechnology, University of Perugia, Via Elce di Sotto, 6, 06123 Perugia, Italy*

ing Γ_2 fixed to the value of 20 μeV. A representative fit of the spectrum of Tel22 at T=277 K is shown in Fig. S2. For each temperature, we noticed that Γ_1 can be described with a constant trend in almost the whole Q range, which is a reasonable behavior suggesting the occurrence of confined random-jump motions. For this reason, we decided to fit Γ_1 with a constant function, but considering only the 0.70 $Å^{-1} \div 1.75$ $Å^{-1}$ Q range because for lower and higher values the quasielastic intensity was quite small and consequently the error bars on Γ_1 were too large, as representatively reported in Fig. S3.

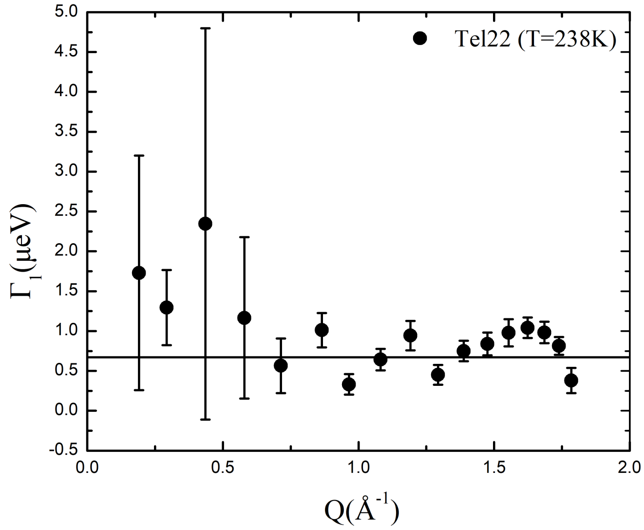

Fig. S3 Q dependence of Γ_1 at a fixed temperature.

Subsequently, we fitted $C(Q)$ using this equation:

$$C(Q) = fA_{12}(Q) \tag{2}$$

via the independent parameters d_2 and f, as reported in Fig. S4.

The function $A_{12}(Q)$ takes the form:

$$A_{12}(Q) = \frac{1}{2}\left(1 - \frac{\sin(Qd_2)}{Qd_2}\right) \tag{3}$$

These parameters were then fixed in the subsequent fit of $A(Q)$ using this equation:

$$A(Q) = (1-f)A_{01}(Q) + fA_{02}(Q) \tag{4}$$

via the independent parameters d_1 and p'_1 (since we have the constraint $p'_2 = 1 - p'_1$) as reported in Fig. S5. The explicit expression for $A_{01}(Q)$ and $A_{02}(Q)$ are:

$$A_{01}(Q) = 1 - 2p'_1p'_2\left(1 - \frac{\sin(Qd_1)}{Qd_1}\right) \tag{5}$$

$$A_{02}(Q) = 1 - \frac{1}{2}\left(1 - \frac{\sin(Qd_2)}{Qd_2}\right) \tag{6}$$

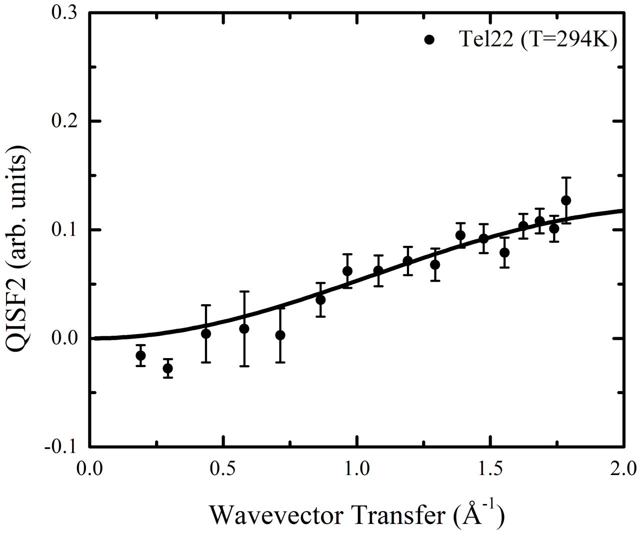

Fig. S4 C(Q) along with the fitting curve using Eq. 2.

The values of the parameters d_1 and d_2 were obtained by first fitting $A(Q)$ and $C(Q)$ for the spectra at the three highest temperatures (in the case of Tel22-Berberine only the spectrum at 280 K was used for this purpose) and, since the results appeared to be independent of temperature, their values were fixed to the average of these three values (or equal to the value at 280 K in the case of Tel22-Berberine) and the fit was repeated for all the temperatures, now varying only the parameters f and p'_1.

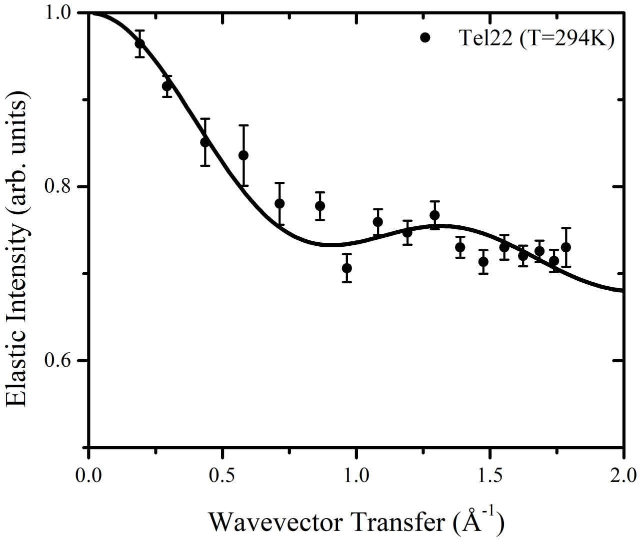

Fig. S5 A(Q) along with the fitting curve using Eq. 4.

3 Additional figures for EINS fitting procedure

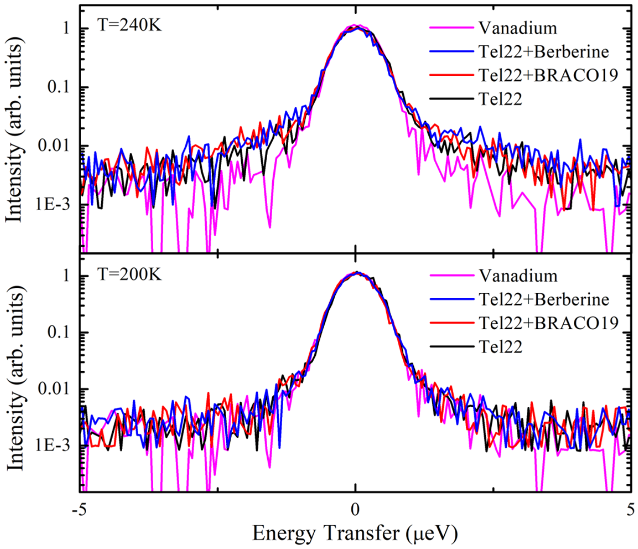

Fig. S6 Comparison between the spectra of the Vanadium standard (magenta) and Tel22 (black), Tel22-Berberine (blue), Tel22-BRACO19 (red). At T= 200 K (bottom) the spectra of the three samples are superimposed to that of the Vanadium standard, thus showing that the quasielasticc signal is negligible. This is not the case at T=240 K (top), where a quasielastic broadening appears.

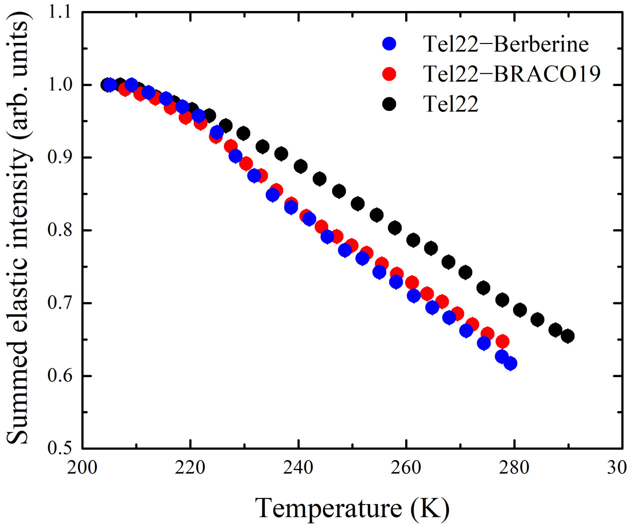

Fig. S7 Summed elastic intensity of Tel22 (black points), Tel22-Berberine (blue points), and Tel22-BRACO19 (red points). A dynamical transition is clearly visible at around 235 in Tel22 alone; complexation causes this transition to take place at a temperature about 15 K lower.

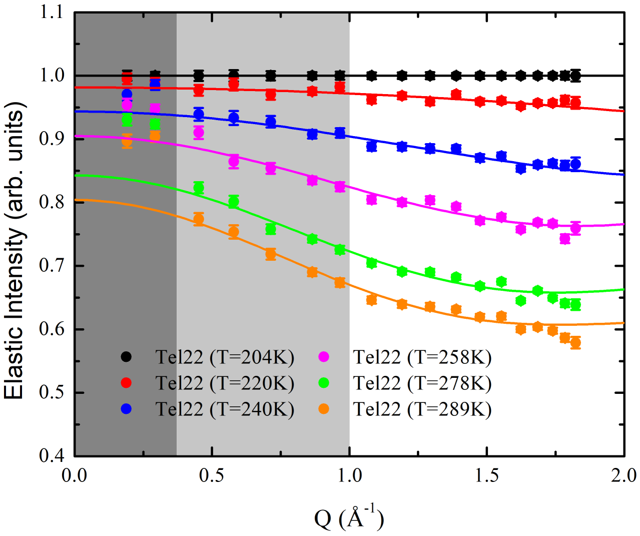

Fig. S8 Example of the fitting procedure of the elastic intensity using Eq. 4 of main text. The light grey region shows the Q range used to initialize the parameters with a Gaussian fit. Points in the dark-grey area were discarded from the fit.

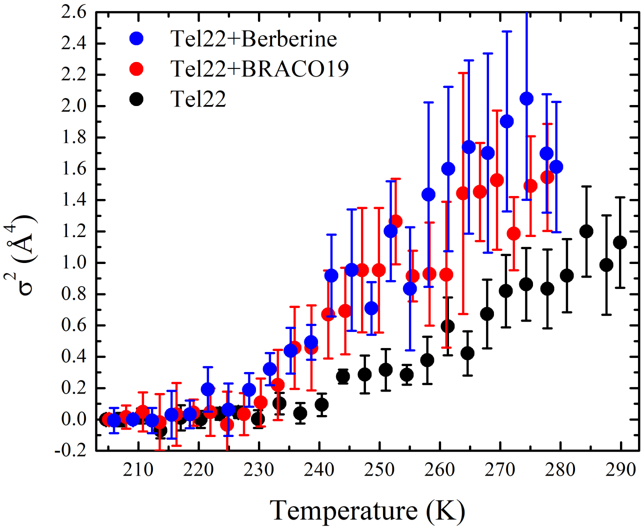

Fig. S9 The standard deviation of the individual MSF extracted from the fit to the elastic intensity using Eq. 4 of the main text for Tel22 (black points), Tel22-Berberine (blue points) and Tel22-BRACO19 (red points).